SPE-201641-MS

Near-Wellbore Deposition of High Conductivity Proppant to Improve Effective Fracture Conductivity and Productivity of Horizontal Well Stimulations

C. Mark Pearson, Liberty Resources; Garrett Fowler, ResFrac; K. Michelle Stribling, Proptester; Jeromy McChesney, Liberty Resources; Mark McClure, ResFrac; Tom McGuigan, US Ceramics; Don Anschutz and Pat Wildt, PropTester

This paper was prepared for presentation at the SPE Annual Technical Conference & Exhibition originally scheduled to be held in Denver, Colorado, USA, 5 – 7 October 2020. Due to COVID-19 the physical event was postponed until 26 – 29 October 2020 and was changed to a virtual event. The official proceedings were published online on 21 October 2020.

Abstract

In conventional formations it has long been established that designing fracture treatments with improved near-wellbore conductivity generates improved production and economic returns. This is accomplished by pumping treatments with increased proppant concentration in the final stages (the traditional proppant ramp design), and in some cases by changing proppant size or type in the final stages to effect greater near-wellbore conductivity - commonly referred to as a "tail-in" design. These designs overcome the impacts of greater near-wellbore pressure loss during production caused by flow concentration in the near-wellbore region compared to distal parts of the fracture.

For vertical wells and crosslinked fracture fluid treatments, the fluid flow and suspended proppant transport is effectively "piston" flow and it was a relatively straight forward matter to engineer the near-wellbore region with a tail-in of higher conductivity proppant. For unconventional reservoirs, with multi-stage horizontal completions using slickwater fluids, it has not been obvious how best to create this improved near-wellbore conductivity and most operators have employed a "one size fits all" strategy of pumping a single proppant type unless there was perhaps a need for flowback control in which case a resin coated proppant might be used as a tail-in.

This paper reports the results of two projects to address the engineering of the near-wellbore fracture conductivity for horizontal well fracturing. Firstly, a series of laboratory tests were run in a 10 ft. × 20 ft. slot wall to visualize near-wellbore proppant duning and layering associated with both "lead-in" and "tail-in" designs. The impacts of these depositions were then quantified using a 3D hydraulic fracture / reservoir simulation code for a variety of stimulation designs in the Middle Bakken and Three Forks formations of the Williston Basin.

The results of this work show that well stimulation treatments in liquid-rich unconventional formations would benefit from a combination of small (5 to 10%) lead-ins and tail-ins of high conductivity ceramic proppant. This minimizes the effects of radial flow convergence in the transverse fractures generated from

the horizontal well and maximizes the economic benefit of the well stimulation. In addition to paying out the small cost increase in only 1 to 2 months, the proppant bands of higher conductivity ceramic help mitigate the effects of longer-term sand crushing and degradation on near-wellbore plugging and thus increases 3-year cumulative free cash flow and the Estimated Ultimate Recovery (EUR) of the well.

Introduction

At the start of hydraulic fracturing in the 1940's, the first experimental fracture treatments did not use proppant. It quickly became apparent that an unpropped fracture healed and a solid material was needed to be injected to facilitate production from the reservoir and to prevent the fracture faces from closing (Howard and Fast, 1970). One of the earliest proppants used in the 1950's was sand dredged from the Arkansas River. Later, it became evident that productivity could be improved by use of screened and processed sand. Monocrystalline sand was used from the Saint Peter formation near Ottawa, Illinois. Referred to as "white" or Ottawa sand, the mined sand consists of grains that are single quartz crystals that offer superior strength properties compared to other sands. With the rapid increase in the number of fracturing treatments, increased proppant demand warranted additional supplies. In 1958, "brown" sand quarries were opened in the Hickory sandstone formation near Brady, Texas. These sands are polycrystalline and each grain is composed of multiple crystals bonded together. The existence of cleavage planes within each grain results in greater proppant crush and reduced strength properties.

By the 1970's, another issue facing industry was the exploitation of deep gas reservoirs that required hydraulic fracturing for successful commercialization. This was addressed when Exxon Production Research invented the use of ceramic proppants by sintering pellets of bauxite – an alumina-silicate clay containing over 80% Al_2O_3 (Cooke et al., 1978). First commercial production of bauxite proppant occurred in 1979 for the exclusive use of fracturing deep gas wells. This was followed in 1982 by the introduction of an Intermediate Strength Proppant (ISP) which is manufactured from a raw material having around 70% Al_2O_3 (Fitzgibbon, 1984). These two products found wide application in vertical conventional gas wells at greater than 10,000 ft. depth.

The many problems associated with the brittle failure of quartz spawned development of an improved sand-based product. Resin coated sand (RCS) proppants were introduced using a phenolic resin coating to encapsulate each sand grain. The resin improves the properties of the sand by reducing the grain angularity and the amount of crush by distributing the load more evenly and encapsulating the fines in the resin coating (Graham, 1975; Johnson and Armbruster, 1984).

In 1985, the first light weight ceramic (LWC) proppant was introduced having an Al_2O_3 content around 50% (Lunghofer, 1985). While not as strong as a bauxite or ISP proppant, it has similar density to sand yet greater sphericity and improved strength.

With the rapid growth in unconventional horizontal well completions the amount of proppant pumped in North America increase rapidly in the period 2010-2020 (Weijers et al., 2019) with the result that just in the past two years over 30 new Brown Sand proppant mines opened – primarily in west Texas – with a capacity of over 100 Million tons/year (Olmen, 2019). Brown Sand, White Sand, Resin-Coated Sand, and Ceramics remain the four main types of proppant available for hydraulic fracturing and are produced in a variety of sizes from 12/18 mesh to 100 mesh.

For conventional formations with vertical wells, industry found that the most important factor for proppant selection is to match the strength of the proppant material to the closure stress of the formation acting on the proppant grains. Figure 1 shows a graphical representation of proppant type selection as a function of closure stress.

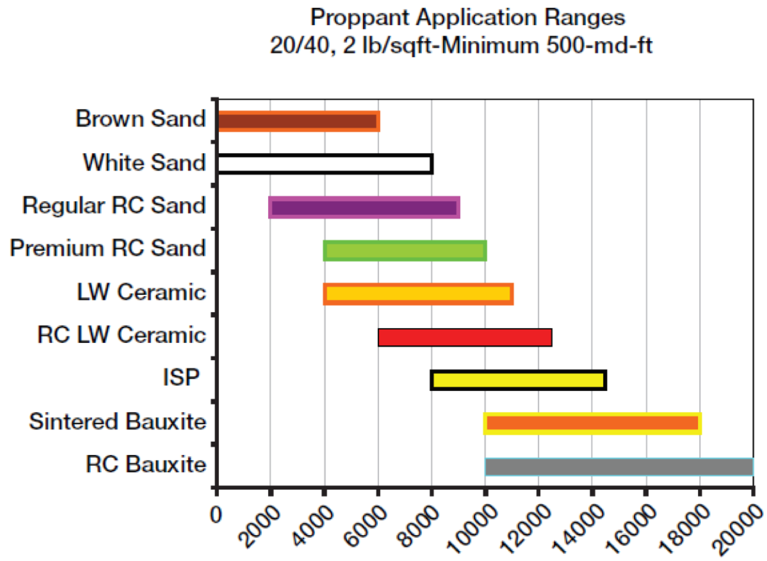

Figure 1—Selection of Proppant Type as a Function of Closure Stress (Economides and Martin, 2007)

The development of unconventional formations with horizontal wells initially started from the application of conventional formation fracturing principles. Some early attempts to cut costs also re-tested omitting all proppant from the treatment (Mayerhofer et al, 1997). Production benefits were not lasting and Coulter et al. (2004) first showed that increasing proppant volumes in unconventional horizontal well stimulations led to a significant increase in early-term production. This trend of increasing proppant volumes per well has been vigorously pursued by industry with the result that proppant loadings being pumped in most unconventional formations are now measured in the 1000’s lbm per foot of lateral (Weijers et al., 2019).

Following the oil price collapse of late-2014, industry has extended the design philosophy of pumping greater volumes of lower quality proppants such that Brown and White Sand proppant are routinely now pumped in formations having closure stresses as high as 10,000 psi (Melcher, 2020). However, this "one size fits all" philosophy of pumping a single type of proppant material fails to comprehend the fracture conductivity needs in the near-wellbore region where flow convergence effects in the transverse fracture will cause the greatest unit pressure drop. Neither does it address the long-term effects of proppant degradation and sand fines migration / plugging of the proppant pack which will be especially severe for sand proppants applied at closure stress above ~7000 psi.

There are some exceptions in design strategy as a small number of operators pump ceramic tail-in designs. Yet another application is what has been called "CounterProp" slickwater fracturing in which the largest and most conductive proppant is pumped first as a lead-in material in order to settle and place higher conductivity proppant near-wellbore. This design strategy was first observed in the laboratory by Kern et al. (1959) who observed that the first proppant pumped in a waterfrac treatment was left closest to the well. Handren and Palisch (2007) document using a lead-in of ceramic proppants in slickwater treatments of the Cotton Valley formation of east Texas with a 20% uplift in IP and a 14% increase in 180-day production; and after two-years of production the projected increase in EUR for the wells ranged from 20-30% (Palisch et al, 2008). Positive results have also been presented from the application of CounterProp designs in a number of basins including the Uintah, Paradox, and Permian Basins, and the Eagle Ford formation (Ely et al; 2019).

The impact of long-term proppant degradation has been investigated by others. Figure 2 shows the results of a 24-well Eagle Ford pilot employing a ceramic tail-in design in half of the wells to mitigate long-term crush effects and fines migration / plugging from sand proppant. As could be predicted from laboratory testing, once the effective closure stress on the proppant pack exceeds ~7000 psi there is considerable production loss associated with the all sand fracture design.

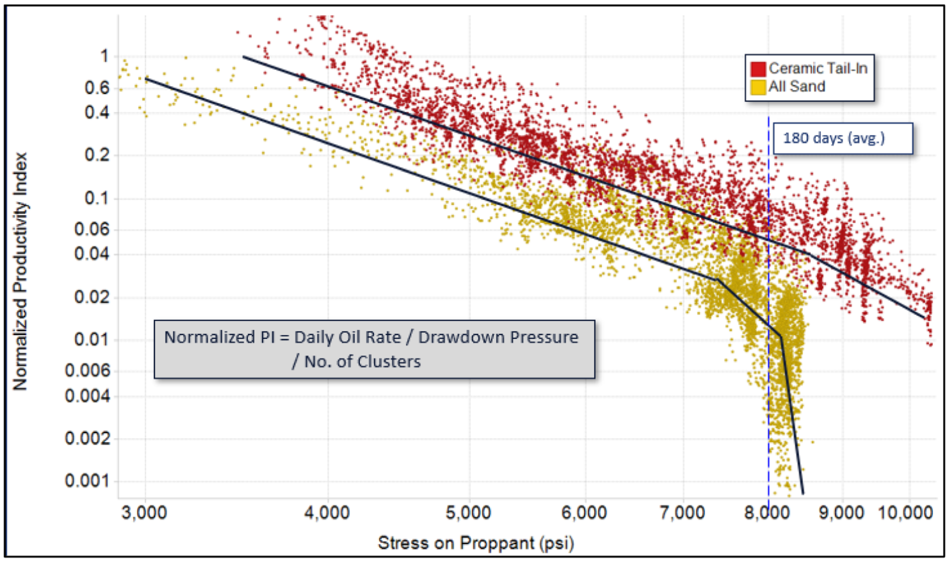

Figure 2—Normalized Productivity Results for Two Eagle Ford Treatment Designs With and Without a Ceramic Tail-In (Al-Tailji, 2018)

The study presented in this paper builds on both the CounterProp design and the effects of longer-term proppant crushing by showing that the engineering of near-wellbore conductivity through the use of both a ceramic lead-in and tail-in will generate the greatest production and economic return from a horizontal well. The flow convergence effects in the early-time flow period means there is immediate (1 to 2 month) payout of the ceramic lead-in and tail-in material while the existence of a high conductivity channel in/above the proppant pack provides longer-term benefits over the life of the well to mitigate the significant degradation of sand proppant due to extended-time crushing and release of fines which plug the proppant pack.

The principle of proppant selection as a function of formation closure stress developed for vertical conventional well fracturing (Figure 1) is just as applicable to the near-wellbore region of a horizontal well production system and there is lost economic opportunity by not engineering the needs of the near-wellbore compared to the body of the fracture.

Proppant Testing

Numerous industry texts have addressed the plethora of laboratory measurements that can be made on fracturing proppant and it is beyond the scope of this paper to discuss them all (Duenckel et al, 2017; Miskimins, 2019). However, the two most important tests affecting the physical properties of the proppant and its application at different closure stresses are the measured crush and fracture conductivity.

The proppant crush test was initially standardized by the American Petroleum Industry (API) in API RP 56 (1983/1995) and API RP 60 (1989/1995), and later in API RP 19C (2007) and API STD 19C (2018). This defines a standardized crush cell in which a 4 lb/ft^2 loading of sieved proppant is placed in the cell and then ramped up to stress over a 1 minute period followed by 2 minutes of holding constant stress. The re-sieved proppant analysis then gives the percent of material falling through the bottom sieve as a % crush. Often reported is the K-factor of the proppant – the stress level at which no more than 10% of proppant is crushed and falls through the bottom screen. Many engineers will use K-factor as a design guide and will not pump proppant having a >10% crush at the given level of closure stress in the formation.

Clearly, while a 3 minute crush test or a difference in K-factor can give a relative comparison between proppant types or sizes, this will have very little correlation to the long-term in situ crush occurring in the reservoir over the 30+ years of productive life of a well. Table 1 shows the results of three commonly used proppants where the crush test is extended to 50 hours. As can be seen, all proppants release more fines with time, and of particular concern is that most of the sand proppants measure >10% fines with as little as 24 hours of stress.

Table 1—Proppant Crush Measurements over Extended Time at 7500 psi for Three Common Proppant Types at Loadings of 1 to 4 lb/ft²

Product	Loading	2 Minutes	10 Minutes	1 Hour	24 Hours	50 Hours
Brown Sand	4 lbs/ft^2	5.64	6.83	6.98	8.31	9.38
White Sand	4 lbs/ft^2	2.91	2.96	3.23	4.25	4.20
Light Weight Ceramic	4 lbs/ft^2	1.26	1.34	1.51	1.85	1.78
Brown Sand	2 lbs/ft^2	9.46	9.95	10.72	14.06	14.17
White Sand	2 lbs/ft^2	5.01	5.13	5.29	6.52	7.70
Light Weight Ceramic	2 lbs/ft^2	2.27	2.41	2.79	3.06	3.51
Brown Sand	1 lb/ft^2	13.58	13.47	14.12	18.21	18.59
White Sand	1 lb/ft^2	8.10	8.87	9.06	10.42	10.63
Light Weight Ceramic	1 lb/ft^2	3.86	4.11	4.99	5.37	5.63

Of significance too is that multiple researchers have shown that cyclic stressing associated with shut-in events over the life of a well can have significant impact on proppant performance (Milton-Tayler, 1993; Duenckel, 2017).

Fracture conductivity data are also obtained from relatively short-term laboratory measurements. The initial API RP 61 issued in October 1989 followed a concerted industry effort to standardize on a short-term testing procedure utilizing a standardized linear flow testing cell. Tests under this procedure lasted for two hours at ambient temperature between steel platens (API RP 61, 1989).

This conductivity procedure was quickly augmented (and later standardized in the procedures of API RP 19D, 2008; and ISO 13503-2:2006) into a long-term testing procedure in which each stress condition in the linear flow cell is held for fifty hours at 250°F between Ohio sandstone platens utilizing oxygen-free, silica saturated 2% KCl. Test results thus generated give the industry a standard set of Conductivity Vs. Stress curves as shown in Figure 3 for the two proppants considered in this simulation analysis. These curves are often referred to as the Reference Conductivity since they are obtained under standardized laboratory conditions with only 50-hours of time at each measured stress level.

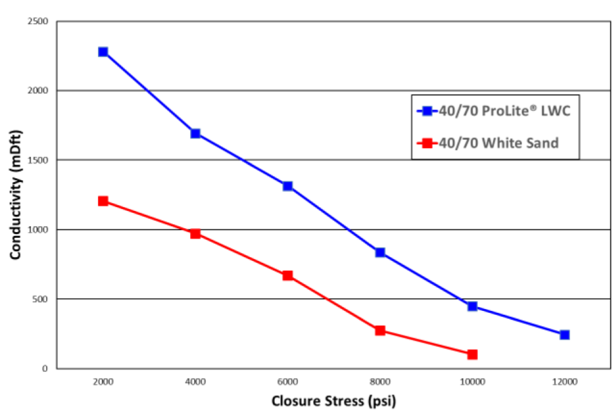

Figure 3—Reference Conductivity Values for 40/70 mesh White Sand and Light Weight Ceramic (Published Data from Covia and US Ceramics)

A major short-coming of any laboratory testing procedure is trying to replicate the conditions over the life of a 30-year well in the time scale over which measurements can be made. Relatively few studies have been conducted of extended-time performance of proppants, but all results show significant degradation with time (Becq et al, 1984; Cobb and Farrell 1986; Much and Penny, 1987 Montgomery and Steanson, 1985). One of the more recent long-term studies was published by Handren & Palisch (2007). Their data gathered over a period of 40 days of constant stress are reproduced in Figure 4.

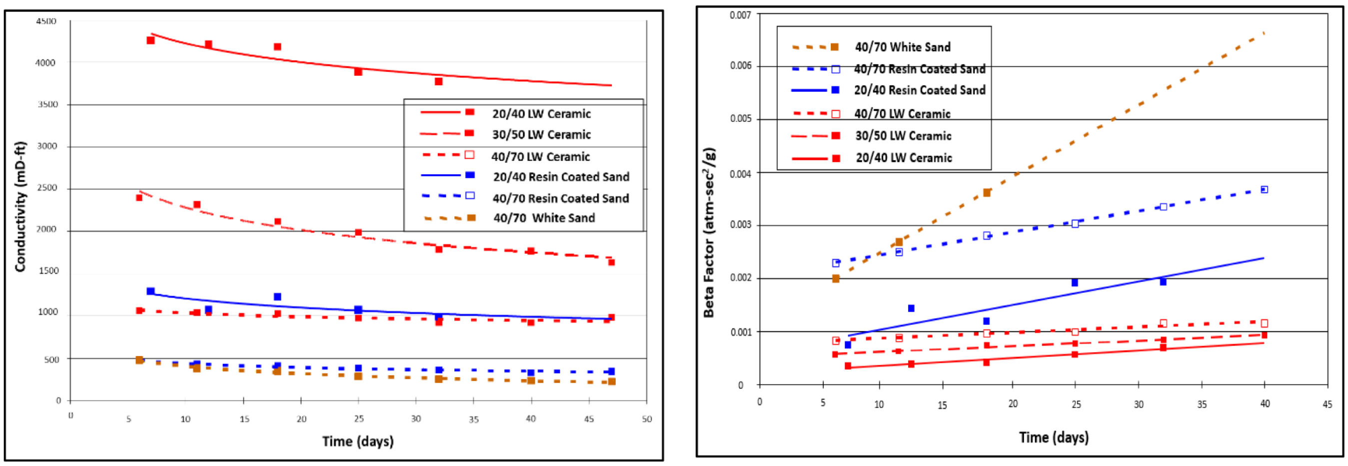

Figure 4—Laboratory Test Results on a Variety of Proppants Holding 6500 psi for 40-days (after Handren and Palisch, 2007)

Of particular note for the two proppants used in the current simulation analysis is that 40/70 white sand lost 53% of its conductivity and had a 230% increase in Beta Factor (the Coefficient of Inertial Flow) over the 40 days of constant stress testing at 6500 psi. 40/70 Lightweight Ceramic recorded a 10% loss in conductivity and a 40% increase in Beta Factor over the same time period. Since conductivity loss is a function of pellet strength, it is reasonable to assume that Brown Sand proppant would lose even more than the 53% conductivity loss reported for 40/70 white sand. However, as yet, the authors are not aware of any extended-time conductivity test data reported on Brown Sands.

The reasons for such significant changes in measured properties with time can be directly related to the strength of the proppant pack and the type of fines released when it crushes. Table 2 gives the crush for Brown Sand, White Sand and Light Weight Ceramic as measured by the 3-minute duration API crust test procedure at 6500 psi. Also detailed is the mass breakdown of the fines into different sieve sizes. Of note is that the White Sand and Brown Sand proppant had 4x and 6x the amount of potentially mobile fines compared to the ceramic. Mobile fines are typically defined as material finer than 200 mesh in size. This significantly larger amount of mobile fines material results from the shattering of the sand grains and has the potential to cause significant plugging in the proppant pack as production fluids transport the fines into the near-wellbore region.

Table 2—Fines Evaluation from API Crush Tests at 6500 psi for Three Common Proppant Types

	40/70 LW Ceramic	40/70 Williston White Sand		40/70 Kermit West Texas Brown Sand	
API Crush	1.0%	1.9%		4.3%	
US Mesh Sieve	Grams Retained	Grams Retained	Mass Comparison to LWC	Grams Retained	Mass Comparison to LWC
80#	0.13	0.22	1.7X	0.52	4X
100#	0.10	0.14	1.4X	0.32	3.2X
140#	0.10	0.15	1.5X	0.32	3.2X
200#	0.06	0.10	1.7X	0.15	2.5X
Pan	0.03	0.12	4X	0.18	6X
Total	0.42	0.73	1.7X	1.49	3.6X

Finally, even under the extended test procedures such as those reported in Figure 4, another element of concern is that "fresh" fluid is circulated with every test measurement. i.e. any fines being generated are flushed out of the cell and the impacts of fines migration and plugging is never measured. In reality, such fines generation is likely to cause significant proppant pack plugging. It is the industry's experience that the combination of increased crush and fines plugging results in *actual* effective conductivity of a fracture pack over time being just a few percent of the reference conductivity measurements made over the 50-hours duration of the API conductivity test carried out under the pristine conditions present in the laboratory. The actual fracture conductivity can be the equivalent of having a Damage Factor of >95% applied to the 50-hour reference conductivity values obtained in the laboratory (Barree et al, 2003; Palisch et al., 2007; and Vincent, 2009).

Fracture Flow Modelling Using Laboratory Proppant Data

Pressure drops from fluid flowing through the fracture proppant pack are a combination of both viscous and inertial effects – i.e. what is often referred to as Darcy and non-Darcy flow. Even in unconventional or low permeability reservoirs, non-Darcy pressure losses resulting from multiphase flow conditions can be an order of magnitude greater than viscous pressure drops predicted by Darcy's equation (Cooke 1975; Vincent et al. 1999; Handren et al. 2001; Pearson 2002; Vincent 2002).

The total pressure drop in the fracture is calculated by the Forchheimer equation (Forchheimer, 1901) as:

$$\left[\frac{\mathrm{d}p}{\mathrm{d}l}\right] = \frac{\mu v}{k} + \beta \rho v^2 \tag{1}$$

where k if the proppant permeability and β is the coefficient of inertial flow.

Calculating the conductivity in the fracture pack under actual downhole producing conditions requires taking reference laboratory data and then accounting for a number of conductivity reduction mechanisms. Duenckel (2017) gave the list of factors for consideration as:

- Proppant pack mass/area concentration - *concentrations lower than the 2 lb/ft² measured in the laboratory will have lower conductivity*.
- Closure stress - *reservoir pressure and drawdown, and stress cycling during production operations*.
- Proppant strength and size - *low strength materials will fail prematurely over higher strength proppants*.
- Gel filter cake and residue damage - *anything impacting proppant pack porosity will reduce conductivity including fines migration/plugging*.

- Velocity and pressure gradient available in the fracture - *convergence effects in horizontal well systems*.
- Time-dependent conductivity degradation – *the recognition that laboratory tests are short-term in nature*
- Capillary and gravity forces – *acting on the fluids in the fracture*
- Multi-phase flow – *relative permeability and multi-phase flow occurs in all fracture systems as opposed to the single-phase measurements made in the laboratory*.
- Inertial, non-Darcy pressure losses – *which are especially significant in gas wells or liquid wells operating at a bottomhole flowing pressure below bubble point*.

Each of these factors has the potential to significantly degrade proppant conductivity from the reference values measured in the laboratory.

Specific to the design of unconventional, horizontal well completion designs, the flow convergence into the lateral needs to be considered and is of great significance to the need for conductivity in the near-wellbore region. For any horizontal well system employing a completion design generating transverse vertical fractures there will be a flow convergence effect as fluid moves from the body of the fracture to the wellbore. If we consider a typical Middle Bakken well landed in the center of the 80 ft. gross thickness of interval then since velocity will increase proportional with the decrease in radial distance from the well, the geometry dictates that × ft/sec of flow in the fracture body increases some 40 to 160 times × ft/sec depending on whether the fracture initiates from the tip or base of the perforation tunnel before entering the 6" diameter wellbore. Thus a fluid velocity change of approximately two orders of magnitude occurs between the body of the fracture and the near-wellbore region – and since the non-Darcy pressure drop restricting production is a square function of apparent velocity this can equate to a four-order magnitude change in pressure loss per unit length! For this reason, actual fracture conductivity in the near-wellbore region is a key factor for both maximizing early-time production, and providing longer-term sustained performance as closure stress with time generates more fines material that will reduce the conductivity of the near-wellbore region such that it can become a choke to production over the life of the well.

Laboratory Studies of Near-Wellbore Deposition

To initiate the study of near-wellbore proppant deposition, a series of laboratory tests were conducted with varying proppants and slickwater treatments using a 10 ft. × 20 ft. slot flow "frac wall" (Figures 5 and 6). With respect to current completion trends, 40/70 northern white sand and 50/140 mesh Texas regional sand were pumped with up to 20% ceramic proppant. The experiments included lightweight ceramic proppant (LWP) and intermediate strength ceramic proppant (ISP) and incorporated both 15% ceramic proppant lead-in treatments and 10% lead-in / 10% tail-in ceramic proppant treatments. Each experiment was tested using various inlet ports to represent wellbore/fluid entry at the upper and lower portion of the fracture. The purpose of each test was to identify and analyze enhanced near-wellbore buildup and conductivity. After each test, the overall proppant settlement was observed and areas of mixed proppant were identified before the structure was disassembled for proppant collection. Samples from four separate areas of the frac wall were collected for conductivity analysis. Each sample was evaluated using Point Specific Conductivity Testing at 8,000 psi, 250°F, with a 1 lb/ft^2 proppant loading. The Point Specific Conductivity Test is a 50-hour, single point test that provides reliable data within the experimental error of the API RP 19D Long Term Conductivity Test (Renkes et al., 2017). The proppant deposition and conductivity values were then digitally mapped on pictures of the proppant dune to highlight the increasing near-wellbore conductivity flow areas.

Figure 5—10 ft. × 20 ft. Slot Flow Test: Mid-Test Photo Showing Settled Dune & Proppant/Fluid Moving Left to Right

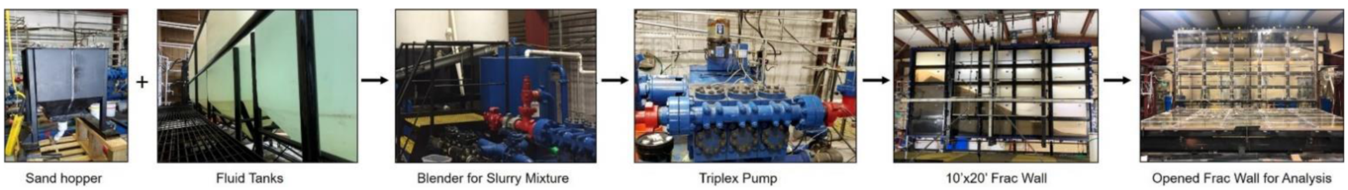

Figure 6—Lab Equipment for 10 ft. × 20 ft. Slot Flow Testing

The laboratory equipment that feeds the frac wall (Figure 6) includes multiple 480-gallon fluid holding tanks, sand hoppers, a centrifugal and a triplex pump, flow loop and in-line densitometer. Frac fluids are mixed in the 160-gallon capacity blender then conditioned using the triplex pump and flow loop until the desired viscosity is reached. Lower rates entering the frac wall requires switching to the centrifugal pump and bypassing the flow loop and triplex pump. Sand is added to the frac fluid on-the-fly prior to entering the 10ft. × 20 ft. frac wall through ¼" inlet ports. Upon the conclusion of the test, the frac wall opens to allow for sample collection. For the purposes of this study, samples were collected and tested on four-stack conductivity machines. Videos of all studies discussed in this paper may be viewed at: http://www.proptester.com/slotflowtesting/

Laboratory Results: Lightweight Proppant Depositions

Experiments were first conducted with 40/70 northern white sand - a product commonly used in the Bakken and Marcellus Shale. To increase near-wellbore conductivity, while respecting cost-conscious completions of operators, 15-20% (by volume) of 40/70 lightweight ceramic proppant (LWP) was incorporated during pumping. Baseline conductivity values were collected on each product prior to slot flow testing. The following diagrams depict the settled dune shape and the conductivity values of various points of the simulated fracture.

15% Lead-In Treatment

Figure 7 maps the proppant settlement and increased near-wellbore conductivity when leading with 15% lightweight ceramic proppant (LWP). LWP traveled nearly halfway across the bottom of the slot flow cell while building a dune peak below the inlet port. Mixed proppant of 40/70 northern white sand and 40/70 LWP settled on top of the ceramic proppant bed, creating a higher conductive flow path around the inlet port. When analyzing reference conductivity samples that were collected from the wall, a 334% increase is calculated when compared to 74 mD-ft at the end of the structure and 321 mD-ft near the inlet (Table 3).

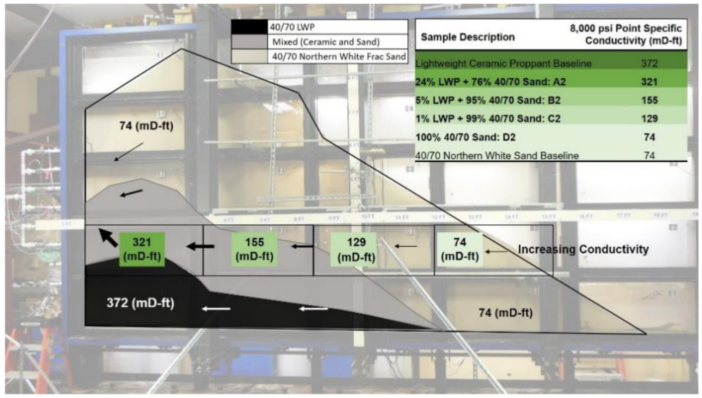

Figure 7—10 ft. × 20 ft. Slot Flow Test Using the Upper Inlets 15% Lead-in with 40/70 Lightweight Ceramic Proppant (LWP) at 0.75 PPA 85% 40/70 Northern White Sand at 1.25 PPA

Table 3—Conductivity Percentage Increase Compared to 40/70 Northern White Baseline (74 mD-ft)

Sample Location	Conductivity Value	Percent Increase
A2: Inlet, Mixed Proppant	321 mD-ft	334%
B2: Mixed Proppant	155 mD-ft	110%
C2: Mixed Proppant	129 mD-ft	74%

10% Lead-in & 10% Tail-in Treatment

This test was conducted with a 10% lead-in and 10% tail-in of 40/70 LWP. Dense, ceramic beds were observed across the bottom of the cell during the lead-in treatment - similar to the previous test. Throughout the tail-in stage, an equilibrium bed height was established and a portion of the ceramic proppant traveled over the dune to create a highly conductive bed on the far side of the peak. Some proppant was blocked as the dune peak fell back into the re-cycle zone and was deposited at the inlet upon shutdown. This treatment allowed for a significant amount of higher conductive proppant to settle at the inlet of the structure (Figure 8). A 188% increase in reference conductivity was measured when comparing samples collected from the lower half of the structure. The ceramic proppant baseline of 372 mD-ft occurred in the near-wellbore region closest to the at the inlet (Table 4).

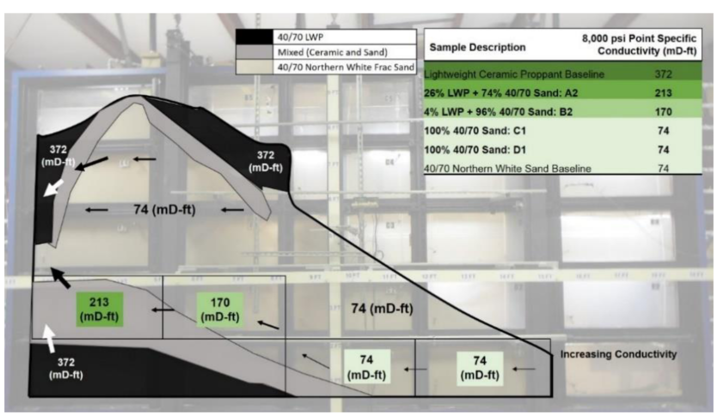

Figure 8—10 ft. × 20 ft. Slot Flow Test Using the Upper Inlets 10% Lead-in with 40/70 Lightweight Ceramic Proppant (LWP) at 0.75 PPA 80% 40/70 Northern White Sand at 1.0 PPA 10% Tail-in with 40/70 Lightweight Ceramic Proppant (LWP) at 1.25 PPA

Table 4—Conductivity Percentage Increase Compared to 40/70 Northern White Baseline (74 mD-ft)

Sample Location	Conductivity Value	Percent Increase
Inlet*	372 mD-ft	**403%**
A2	213 mD-ft	**188%**
B2	170 mD-ft	**130%**

Laboratory Results: Intermediate Strength Proppant Depositions

40/80 intermediate strength proppant (ISP) was tested with 50/140 (100 mesh) Texas regional sand. 100 mesh is commonly used in the Permian Basin and Eagle Ford Shale and the conductivity baseline for this product was tested and recorded as 22 mD-ft for this study. 40/80 intermediate strength ceramic proppant was integrated into pumping to increase near-wellbore conductivity. The same treatment options were applied as the lightweight ceramic proppant.

15% Lead-In Treatment

When pumping a lead-in of ISP, the product created a bed along the bottom of the frac wall. A mixture of the two products was then observed when switching to 50/140 mesh sand and again at the very end of the test. While the conductivity of the ceramic proppant bed at the bottom of the cell can be inferred using the baseline results of 480 mD-ft, samples were collected throughout the structure at the height of the inlet to study the increasing near-wellbore conductivity values (Figure 9). An increase of 373% was calculated when comparing conductivity values of the mixed product at the inlet to the baseline sand value (Table 5).

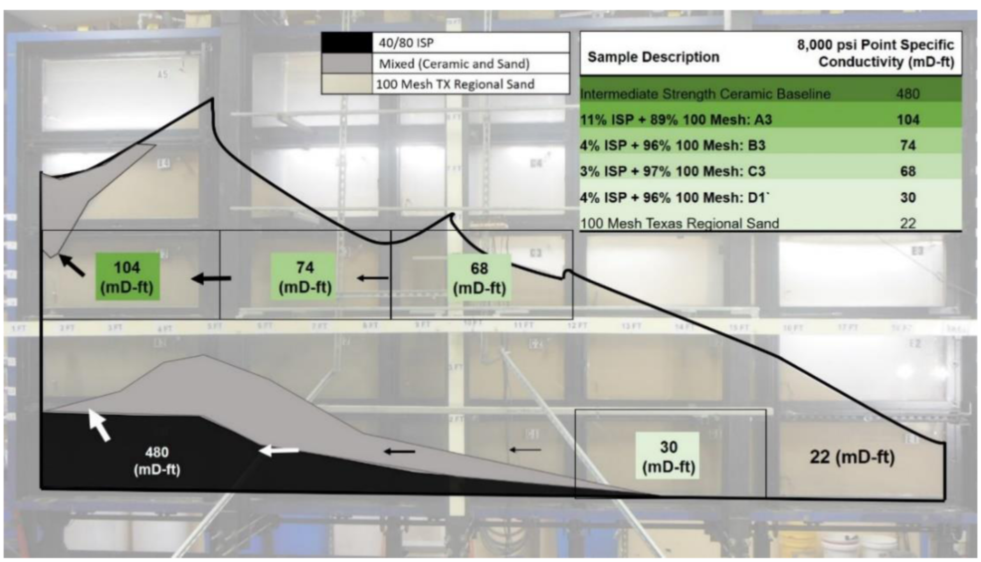

Figure 9—10 ft. × 20 ft. Slot Flow Test Using the Upper Inlets 15% Lead-in with 40/80 Intermediate Strength Ceramic Proppant (ISP) at 0.75 PPA 85% 50/140 Mesh Texas Regional Sand at 1.25 PPA

Table 5—Conductivity Percentage Increase Compared to 50/140 TX Regional Sand Baseline (22 mD-ft)

Sample Location	Conductivity Value	Percent Increase
A3: Inlet, Mixed Proppant	104 mD-ft	**373%**
B3: Mixed Proppant	74 mD-ft	**236%**
C3: Mixed Proppant	68 mD-ft	**209%**
D1: Mixed Proppant	30 mD-ft	**36%**

10% Lead-In & 10% Tail-in Treatment

When pumping a lead-in and tail-in of ISP, the ceramic proppant quickly deposited at the bottom of the cell during the lead-in stage (Figure 10). Mixed proppant deposited on top of the ceramic proppant bed when transitioning to 50/140 frac sand. The pattern was then reversed when switching back to ISP. Less ISP traveled over the top of the dune compared to lightweight proppant. The majority of the sand pumped at the end of the test remained in the re-cycle zone and quickly settled upon shutdown. The samples collected and tested after the experiment showed a 268% increase in conductivity in the panel closest to the inlet. However, with the presence of a significant proppant bed of ISP deposited directly at the inlet port, the baseline of 480 mD-ft at the inlet can be inferred as the conductivity value at the inlet (Table 6).

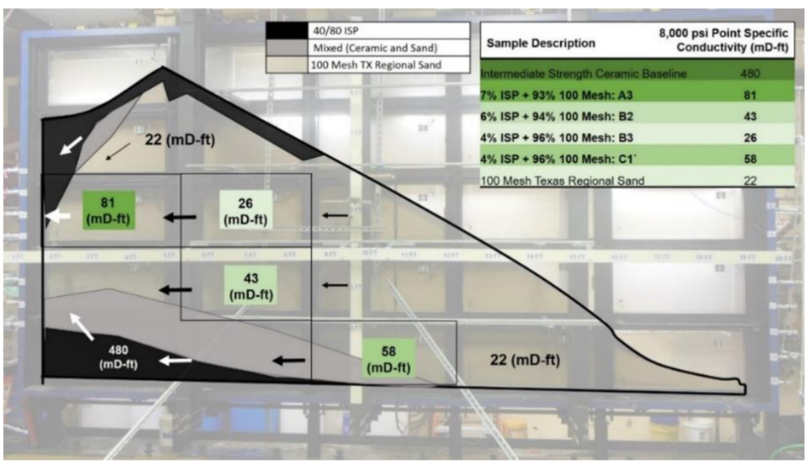

Figure 10—10 ft. × 20 ft. Slot Flow Test Using the Upper Inlets 10% Lead-in with 40/80 Intermediate Strength Ceramic Proppant (ISP) at 0.75 PPA 80% 50/140 Mesh Texas Regional Sand at 1.0 PPA 10% Tail-in with 40/80 Intermediate Strength Ceramic Proppant (ISP) at 1.25 PPA

Table 6—Conductivity Percentage Increase Compared to 50/140 TX Regional Sand Baseline (22 mD-ft)

Sample Location	Conductivity Value	Percent Increase
Inlet*	480 mD-ft	**2,081%**
A3	81 mD-ft	**268%**
B2	43 mD-ft	**96%**
B3	26 mD-ft	**18%**
C1	58 mD-ft	**164%**

Upper Zone Inlet vs. Lower Zone Inlet

Placement of the fluid inlet valves at the side of the frac wall impacts the shape of the dune formation and deposition of the various proppants. Tests were completed with the inlet injection in both the upper half of the structure and near the bottom of the structure to mimic the case of downward and upward fracture growth respectively. Figure 11 shows an example deposition of the ISP combined lead-in and tail-in design from the two sets of injection ports. A difference in dune generation can be observed as the zone of mixed proppant type extends much higher in the case of injection into the lower inlet port reflecting the significant height growth in the dune buildup occurring when height growth occurs above the injection zone. Also, as observed in all tests incorporating a ceramic tail-in, the zone immediately adjacent to the flow entry port/ perforation is filled with higher conductivity ceramic proppant.

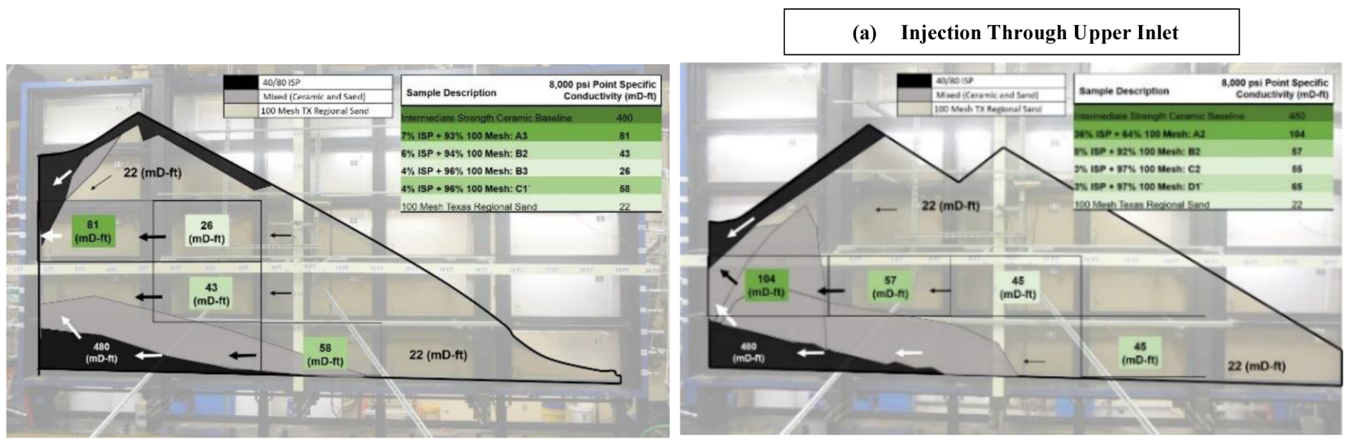

Figure 11(a) and 11 (b)—Comparison of Ceramic Lead-In and Tail-In Designs from Upper and Lower Injection Ports

Consistent proppant transport behavior was observed throughout the study when comparing the treatment options with both of the ceramic proppants that were tested. Significant ceramic proppant beds were deposited along the bottom of the fracwall when leading in with a ceramic proppant stage which when combined with the deposition of tail-in ceramics directly at the inlet ports provide for increased near-wellbore conductivity compared to the frac sand being pumped in the remainder of the tests.

Bakken Geology

The Bakken petroleum system is located in the Williston Basin of North Dakota, South Dakota, and Montana in the United States, and parts of Saskatchewan and Manitoba in Canada (Figure 12). The Williston Basin is a large intracratonic sag basin that was formed between the Wyoming craton to the southwest and the Superior craton to the northeast (Fischer et al, 2005). The deepest part of the basin resides in the center, just north of the Little Knife anticline, with gently dipping beds from the basin margin to the center where depths for the Bakken Formation reach greater than 11,000 ft. TVD. The Williston Basin is structurally quiet with the Nesson anticline being the prominent feature and location of first oil discovery in 1951.

Figure 12—Location of the Williston Basin and Major Structural Features (after Heck, 2004)

The location of the Martin C 158-93-11-2-3MBH Bakken horizontal well described in this paper is located east of the Nesson Anticline and denoted by a red star in Figure 12.

The Bakken petroleum system is made up of the Bakken Formation and Three Forks Formation which are Mississippian and Devonian in age. It is sealed above by the tight limestone of the Lodgepole Formation, and below by the tight dolomites and anhydrites of the Birdbear (Nisku) Formation. The Bakken Formation consists of the Upper Bakken shale, Middle member, and Lower Bakken shale. The Upper and Lower Bakken shales are the source rocks that generate hydrocarbon for the Bakken petroleum system. The Middle member is the primary reservoir target in the basin, along with the upper portion of the Three Forks Formation.

Figure 13 shows the individual lithofacies that make up the Middle member and Upper Three Forks. The Middle member consists of six lithofacies that range from subtidal, silty sandstones to intertidal-shallow shelf, silty dolomites. Reservoir properties are best developed in the latter, where porosities range from 7-10 %, and matrix permeabilities around 0.1 md. The Upper Three Forks consists of five lithofacies that are composed of interbedded, silty dolostones and green, clay rich mudstones.

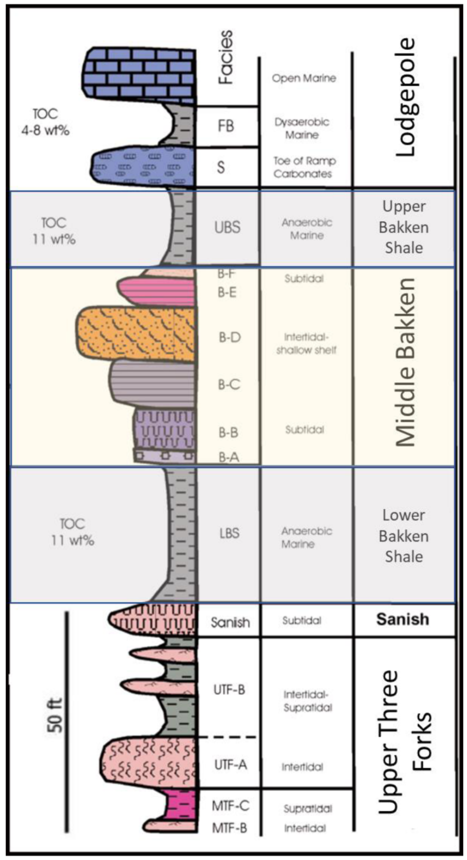

Figure 13—Bakken Lithofacies (after Sonnenberg et al, 2011)

The East Nesson area has the greatest total petroleum system thickness in the Williston Basin (Figure 14) but has lower thermal maturity and reservoir pressures than the deep, center part of the basin. Stock Tank Original Oil in Place (STOOIP) per 1280-acre spacing unit in the East Nesson area averages 28 million barrels of oil for the Middle Bakken and Upper Three Forks combination.

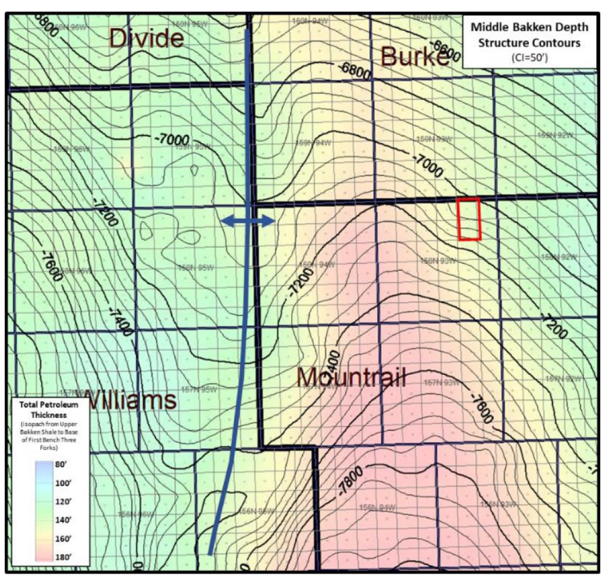

Figure 14—Middle Bakken Depth Structures and Total Petroleum Thickness Color Fill. (The Martin 1280-acre DSU is outlined in red and located in T158-R93, Sec. 2 & 11; Nesson Anticline denoted by blue line)

Martin Drilling and Spacing Unit

The Bakken well example in this paper is the Martin C 158-93-11-2-3MBH (Martin-3MBH) - located just east of the Nesson anticline (Figure 14) in north Mountrail County, North Dakota and is drilled in a 1280-acre drilling and spacing unit (DSU). A pilot hole was first drilled to the Birdbear Formation and an advanced suite of open hole logs were acquired. On the first wireline run a quad combo log suite was acquired including gamma ray, induction resistivity, neutron and density porosity, and dipole sonic. With the dipole sonic data, a full suite of rock mechanics computation was incorporated into the fracture modeling for this study. Wireline run two was a suite of specialty logs including CMR, spectral gamma ray, dielectric, and ECS mineralogy. Computed STOOIP per 1280 DSU from the Martin-3MBH pilot hole was calculated to be 31 million barrels of oil for the Middle Bakken member and Upper Three Forks combined.

The company's current development plan for the area is a 3x3 well plan where three laterals are placed in the Middle Bakken member, and three laterals are placed in the Upper Three Forks. The recovery factor estimated for this area is around 10%. This would allow a recovery around 3.1 million barrels of oil for a fully developed Martin 1280-acre DSU.

A 10,204 ft. horizontal well was drilled from the pilot hole targeting the Middle Bakken member. Figure 15 shows a profile view of the Martin-3MBH horizontal. The lateral drilled up-dip with an average apparent formation dip of 0.77° achieving 80% of the lateral in the seven foot target window. The mud weight averaged 9.7 ppg while drill cuttings showed streaming yellow-white cuts throughout. Figure 15 also shows the 27 geoengineered, hydraulic fracture stages. A successful anti-collision program was implemented, drilling underneath an existing Middle Bakken well, the Nelson 1-11H.

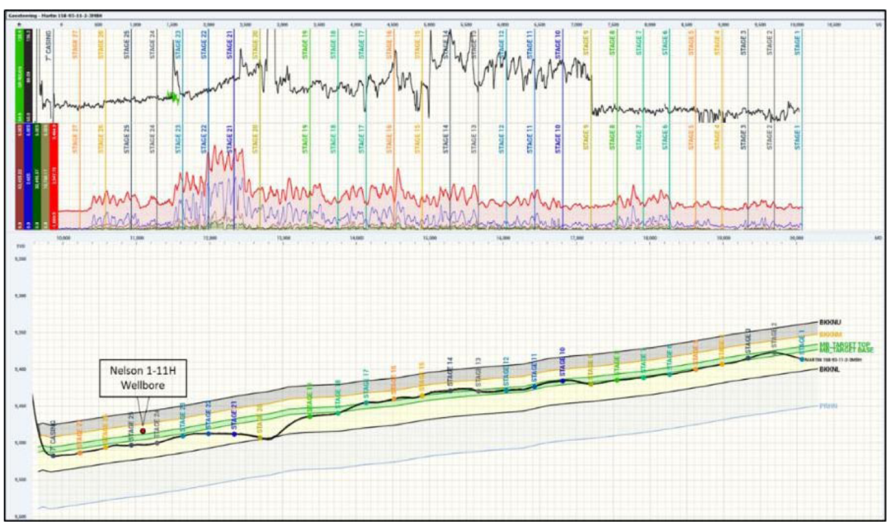

Figure 15—Martin-3MBH Wellbore Profile with Fracture Stages and Location of Anti-Collision Wellbore (Nelson 1-11H). Gamma Ray is in the top track with total gas and C1-C4 in the second track.

Fracture Simulation Model

The ResFrac simulator used for analysis is a fully integrated hydraulic fracturing and reservoir simulator capable of modeling fracturing and reservoir production in a single simulation model (McClure et al., 2020a). The simulator uses a fully coupled approach: all governing equations are solved in every element in every timestep. Quoting from Fowler et al. (2019):

"Mass balance equations are solved for fluid components (water, oil, and gas in the black oil model; or pseudocomponents in the compositional model), water solute components (such as high viscosity friction reducer), and defined proppant types. Mechanical equilibrium equations are solved to calculate stress changes due to crack opening and due to fluid pressure changes in the matrix. The equations are solved in a fully coupled approach; all governing equations are satisfied in every element in every timestep. The hydraulic fractures are meshed as cracks with aperture on the order of microns to millimeters, and the cubic law is used to calculate conductivity. Proppant transport is calculated considering gravitational settling, gravitational convection, hindered settling, bed slumping, proppant trapping, and other effects. As the proppant volume fraction approaches 0.66, the proppant becomes immobilized into a packed bed of particles, and the fluid flow equations transition to equations appropriate for flow through porous media. The flow equations consider relative permeability, gravitational effects, non-Darcy pressure drop, and non-Newtonian fluid rheology. The simulator uses the ‘planar fracture modeling’ approach. In shale, core-across studies show that fractures are complex, with branching and stepovers at small scale (Gale et al., 2018). However, in most formations, field-scale observations such as microseismic and offset well hits indicate broadly linear features."

The ‘proppant trapping’ mechanism built into ResFrac defines how lead-in material may be effective at placing proppant near-wellbore both adjacent to the entry point or even above it in the case of upward fracture growth, in addition to the more commonly modeled settling of proppant to the bottom of the fracture as seen in laboratory tests. As described by Gale et al. (2018) and Maity and Ciezobka (2020), localized proppant screenout can occur at natural fractures and other points of small-scale complexity. In ResFrac, this is captured as a ‘proppant trapping’ mechanism that immobilizes some proppant as it flows through the fracture, and so prevents all the proppant from settling out into a bed along the bottom of the fracture (McClure et al., 2020a; 2020b). With proppant trapping, at least some of the first proppant injected will be trapped near the well. In the simulations performed in this study, proppant transport was complicated by the vertical fracture growth upward into the understressed Lodgepole. The height growth shortened fracture length in the Middle Bakken pay zone, but improved vertical proppant placement by pulling the proppant upward with the vertical flow of the fluid. Despite the height growth, lead-in and tail-in stages were still a good strategy for placing high conductivity ceramic near the wellbore.

History Match of Martin-3MBH Well

To calibrate the model input parameters and investigate the effect of high conductivity proppant on well performance, a simulation model was built and calibrated to the Martin-3MBH well. The subject well was completed using a 20% mass percent tail-in ceramic proppant design.

The simulation model was populated with a 63 layer, geologic, geomechanical, and petrophysical layer-cake property model from the operator. Per best practices outlined in McClure et al. (2020b), fracture toughness was initiated with 1% variance throughout the model domain. To ensure the subject well is not double counting production, matrix permeability further than half-a-well-spacing on either side of the subject well is zeroed out at the beginning of production (this allows fractures to leakoff, but not produce from the region assumed to be drained by an offsetting well). Figure 16 shows the model setup, with gray regions indicating this ‘zero permeability’ region, and SHmax oriented vertically in the page.

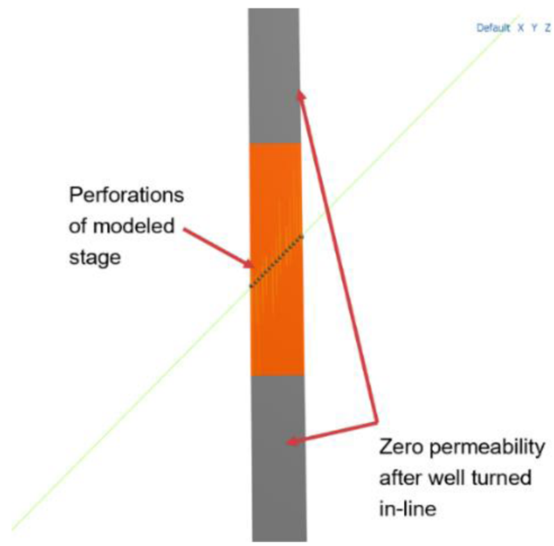

Figure 16—Model layout and setup

The operator then advised on expected fracture geometries (as observed from microseismic) and perforation efficiency (as measured from step down tests), and supplied 1.75 years of production data and calculated bottom hole pressures (BHP). Bottom hole production pressure was used to constrain the model during the production period, such that the model predicted the production rates of the three phases of fluid production.

Two proppants, 40/70 mesh white sand and ceramic proppant were used in the stimulation treatments.

Reference 50-hour conductivity curves were obtained from the supplier data sheets (Figure 3) and then shifted to match the 6500 psi extended time data measured by Handren and Palisch (2007) extrapolated to 180-days. Figure 17 gives the calculated 180-day reference conductivity versus normal stress curves used for the two proppant types at a loading of 2 lbs/ft^2.

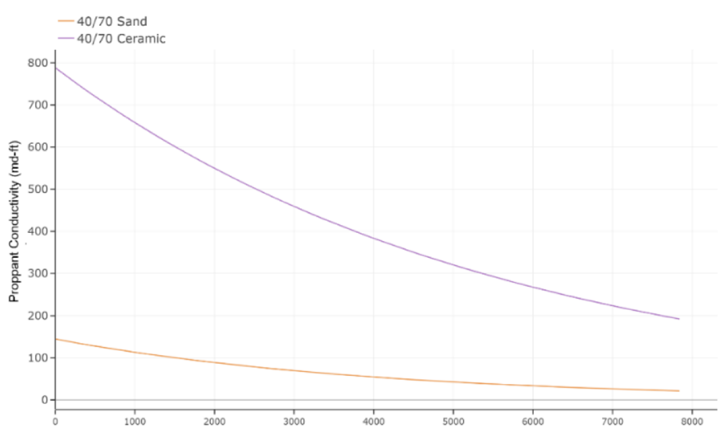

Figure 17—Calculated 180-day Reference Conductivity Versus Normal Stress at 2 lbs/ft^2 for the Two Proppants

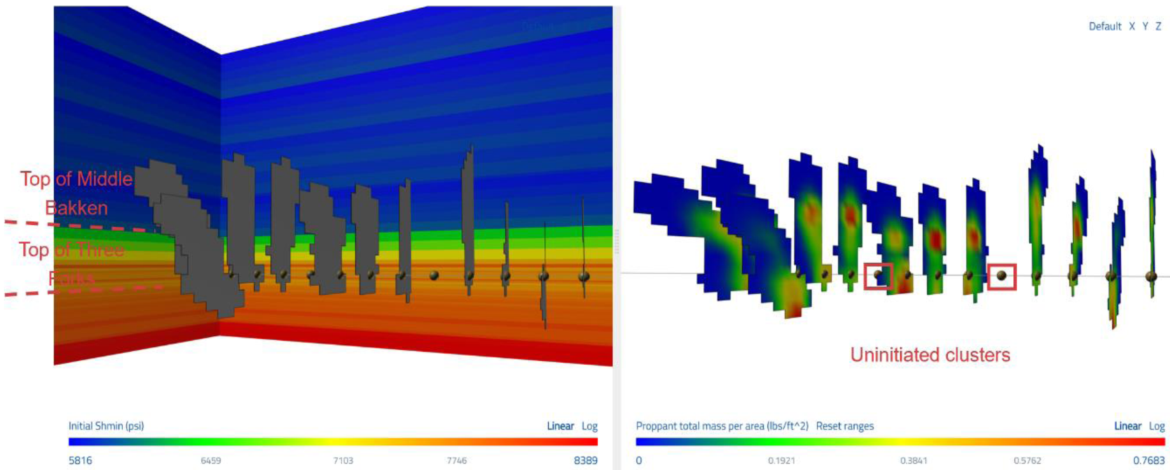

Figure 18—Geometry of History Matched Fractures Showing Height Growth into the Lodgepole Formation and 85% Perforation Cluster Efficiency

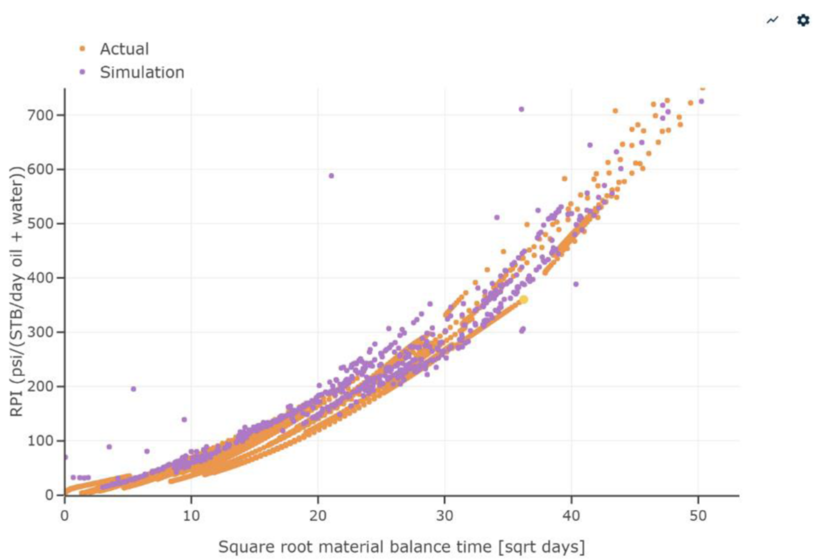

Figure 19—RTA Trends for Actual and Simulated Data. (Oil relative permeability was tuned in the simulation model to match the upward curvature observed in the actual data).

History matching simulation models can be a time consuming and iterative process. Fowler et. al. (2020) outline a streamlined process for matching data using a coupled hydraulic fracture and reservoir simulator. That process, as listed in Table 7, was followed in matching the Bakken historical data for the Martin -3MBH well:

Table 7—History Matching Process (after Fowler et al., 2020)

1. List data and objectives of the history match
2. Set up the model with geologic properties, wellbore and completion designs, and fracturing and production schedules. Add stress observation plane at wellbore depth.
3. Run the initial models using BHP control
4. Use microseismic, frac hit data, DAS, and other data to roughly tune the fracture geometries
5. If available, use step down test, camera, or sonic data to calibrate perf efficiency
6. Add external fracture and tune to match stress shadowing observed in stress observation plane
7. Check that ISIPs and net pressures match field observations within reason
8. Adjust wellbore friction factor to match surface treating pressures
9. Tune relative permeability (endpoints and exponents) to match watercut
   a. Plot relative permeability curves.
   b. Mark your initial water saturation.
   c. Plot water fractional flow.
10. Use RTA to hone in on permeability and fracture conductivity in early-time
11. Adjust relative permeabilities to match GOR behavior
    a. Check 3D image. Is frac pressure = BHP?
12. Use RTA characteristics to identify later-time phenomena
    a. Interference and no-flow boundaries
    b. Dropping below bubble point
    c. Pressure dependent permeability degradation

Microseismic collected by the operator suggested significant height growth from the Middle Bakken into the Lodgepole formation, and overall fracture lengths of 1000-1500 feet. Outcrop and observational studies from industry have indicated that fracture toughness scales nonlinearly with fracture size (McClure et al., 2020b). Significant fracture height into the Lodgepole was achieved in the model using the stress profile supplied by the operator, and desired fracture lengths were achieved by modifying the toughness scaling factor.

Tensile strength was elevated above the default of 0 psi to achieve the 75-85% perforation efficiency seen from step-down testing at the end of each stage.

Production data were matched by adjusting global permeability and relative permeabilities of the three phases. Fowler et. al. (2020) document various RTA trends commonly observed in shale wells. Plotting the RTA for the subject well reveals upward curvature in the RTA trend at late time. The curvature of the RTA corresponds with an increase in the GOR. Oil relative permeability was tuned to match the reduction in oil permeability below bubble point observed in the RTA plot.

The resulting match to the historical data is strong. Figure 20 shows the actual data in dashed trends and the simulated data as solid trends. The history match results in a model that reproduces a tight fit to the actual data as shown in the figure. Note that early-time gas measurements were considered suspect, so early-time GOR was neglected from the history match assessment criteria.

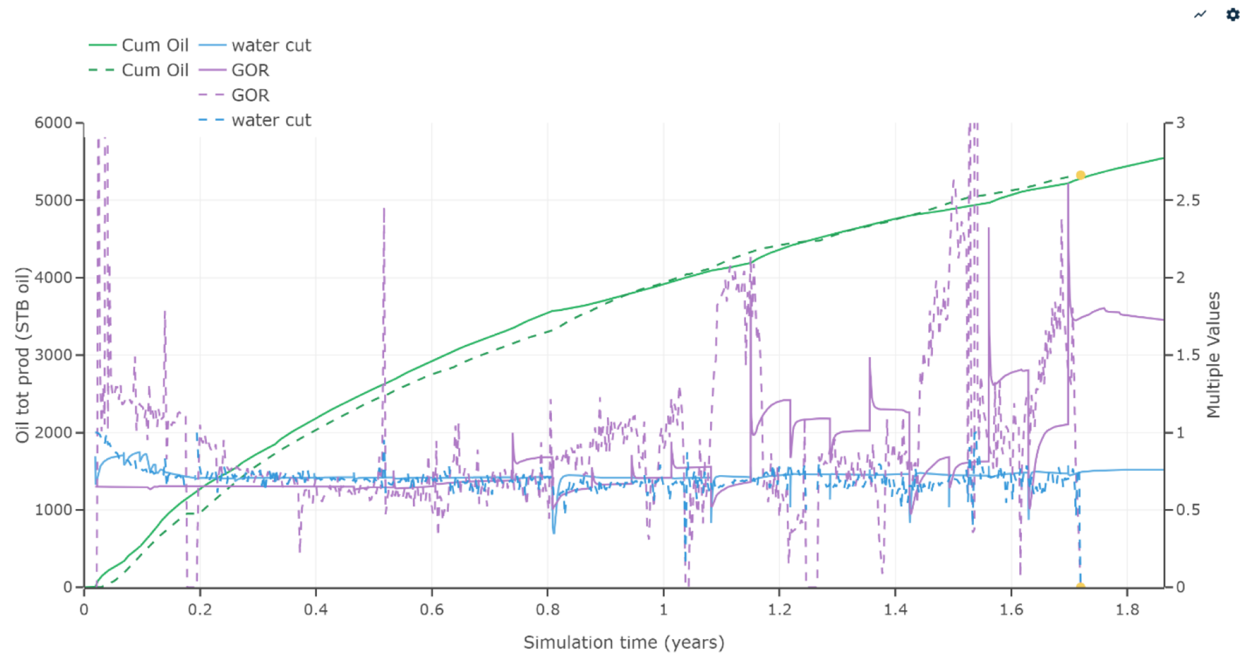

Figure 20—History Matched Production Data for the Martin -3MBH Well. (Actual data plotted as dashed trends, simulated as solid trends).

Middle Bakken Simulation of Lead-Ins and Tail-Ins

Having matched the Martin -3MBH production results, a series of simulations was run investigating what would have been the impact of running a variety of all sand, ceramic lead-in and tail-in designs.

Table 8 gives the specifics of the treatment designs that were run:

Table 8—Simulation Cases

All 40/70 White Sand
95% 40/70 White Sand with 5% 40/70 Light Weight Ceramic Lead-In
90% 40/70 White Sand with 10% 40/70 Light Weight Ceramic Lead-In
80% 40/70 White Sand with 20% 40/70 Light Weight Ceramic Lead-In
95% 40/70 White Sand with 5% 40/70 Light Weight Ceramic Tail-In
90% 40/70 White Sand with 10% 40/70 Light Weight Ceramic Tail-In
80% 40/70 White Sand with 20% 40/70 Light Weight Ceramic Tail-In
90% 40/70 White Sand with 5% 40/70 Light Weight Ceramic Lead-In and Tail-In
80% 40/70 White Sand with 10% 40/70 Light Weight Ceramic Lead-In and Tail-In

For the sensitivity analyses, a stair-stepped Bottom-Hole Flowing Pressure control was applied consistently across all the scenarios investigated. An initial BHFP of 1500 psi was assumed for the first month of production, then 1000 psi until 90 days, and then 500 psi for the rest of the life of well - reflective of a scenario of operating under "pumped-off" rod pump artificial lift conditions.

For all cases, the distribution of proppant could be visualized to see the extent of the impacted area in the near-wellbore region. As an example, Figure 21 shows the spatial distribution of ceramic proppant for the 5% lead-in & tail-in case. As can be observed, most of the ceramic proppant has remained near-wellbore.

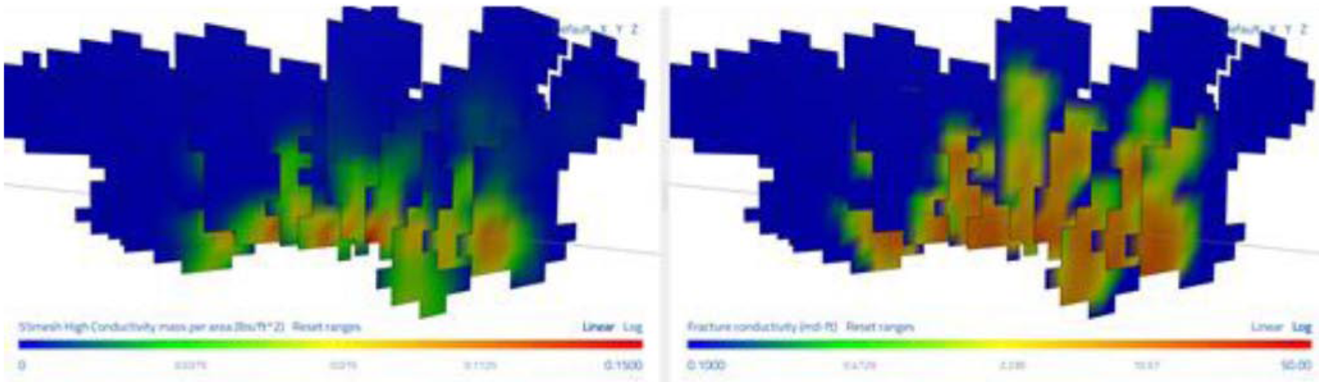

Figure 21—Distribution Of Ceramic Proppant and Fracture Conductivity For The 5% Lead-in & Tail-in Design

Early-Time Production Results

Figure 22 shows the early-time production results for the design cases listed in Table 8. Typically, the first months are the highest productive period in the life of an unconventional well once artificial lift has been run. Near-wellbore pressure drops will therefore be the highest and the consequence of that results in significant benefit to having the near-wellbore region loaded with higher conductivity proppant.

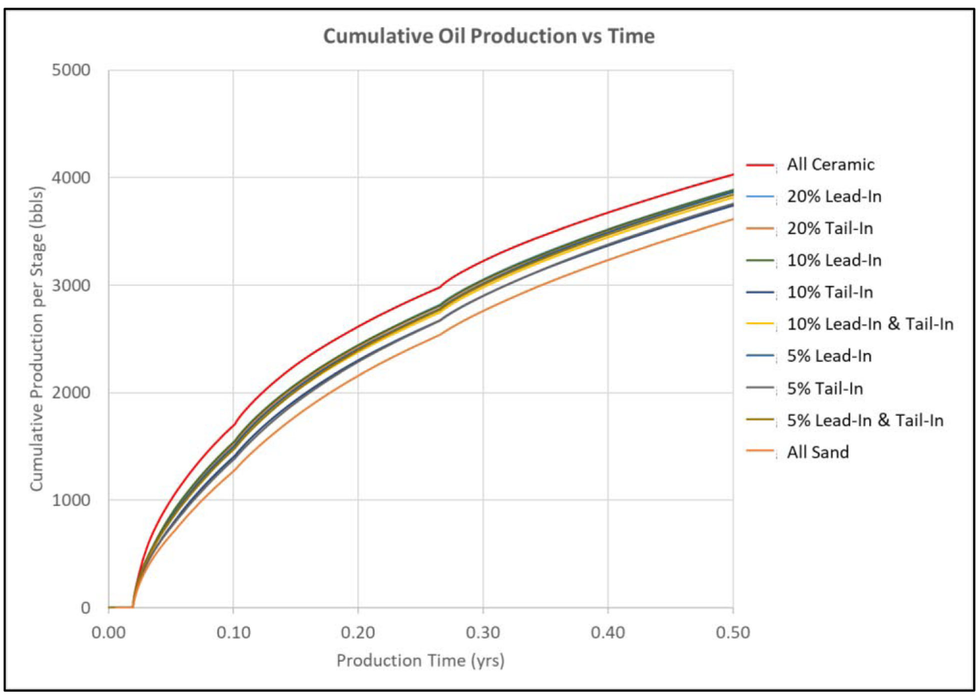

Figure 22—180-Day Cumulative Oil Plots for the Various Designs

Table 9 gives the tabular 180-day cumulative oil results showing that an all ceramic frac generates 12% greater oil production relative to sand – however, the cost of an all ceramic fracture design is not immediately paid-out in the first 180 days. However, the lead-in and tail-in designs provide a significant amount of the total benefit. Notably both the 5 and 10% tail-in only, or lead-in & tail-in designs, provide ~75% of the benefit of an all ceramic treatment. From a pay-out standpoint the small added costs pay-out from 1 to 6 months of increased production.

Table 9—180-day Calculated Cumulative Oil Recovery for Various Fracture Designs

	Sand Pumped (lbs)	Ceramic Pumped (lbs)	Well Cost ($)	Well Cost Increase	Cumulative Oil (bbls)	% Oil Increase Over All Sand Frac	Ceramic Payout Period (Months)
All Sand	10,936,728	-	$ 5,585,180	-	97,671	-	N/A
5% LWC Lead-In	10,389,897	546,831	$ 5,650,800	1%	102,099	5%	1
5% LWC Tail-In	10,389,897	546,831	$ 5,650,800	1%	105,410	8%	1
5% LWC Lead-In & Tail-In	9,843,066	1,093,662	$ 5,716,420	2%	105,321	8%	1
10% LWC Lead-In	9,843,066	1,093,662	$ 5,716,420	2%	101,790	4%	2
10% LWC Tail-In	9,843,066	1,093,662	$ 5,716,420	2%	106,718	9%	2
10% LWC Lead-In & Tail-In	8,749,377	2,187,351	$ 5,847,662	5%	107,880	10%	6
20% LWC Lead-In	8,749,377	2,187,351	$ 5,847,662	5%	108,132	11%	6
20% LWC Tail-In	8,749,377	2,187,351	$ 5,847,662	5%	107,666	10%	6
All Ceramic	-	10,936,728	$ 6,897,588	23%	109,112	12%	N/A

Of note in Table 9 is that for the 5% and 10% cases the same amount of ceramic proppant pumped in the tail-in treatments gave higher recovery than the lead-in designs. We interpret this as being a consequence of the excessive height growth occurring into the non-oil productive Lodgepole zones such that the build-up of the near-wellbore dune during the lead-in is being somewhat wasted compared to the lateral extent achieved with the tail-in volumes being placed in a layered manner and directly next to the wellbore at the end of the treatment.

Production over the Period of Well Pay-Out

For Liberty Resources, the best area in inventory has wells that have EURs from 600-750 MBO over their productive life. Such wells will pay-out in 15 to 18 months. However, in the East Nesson area, where the majority of the company's well inventory exists, predicted EUR's are from 400 to 450 MBO and payout times are 24 to 36 months. For this reason the company tends to focus on well pay-out times and 3-year cumulative free cash flow in order to quantify relative economic performance.

Continued proppant conductivity damage will occur during this extended period of production due to both increased time and exposure. Also, because of the effects of creep and deformation in the overlying strata, with time this will increase the total vertical stress loading back onto the formation. While total horizontal stress is likely still decreasing, the effective horizontal stress on the proppant is increasing due to both the geomechanical creep and the continued drawdown in bottomhole flowing pressure.

To account for these effects causing proppant degradation with time, the simulations were re-run with damage factors of 50% and 90% applied to the sand proppant to account for its differential under-performance with stress and time. Example conductivity spatial distributions after 3-years of production are shown in Figure 23 while the 3-year cumulative production results are shown in Figure 24.

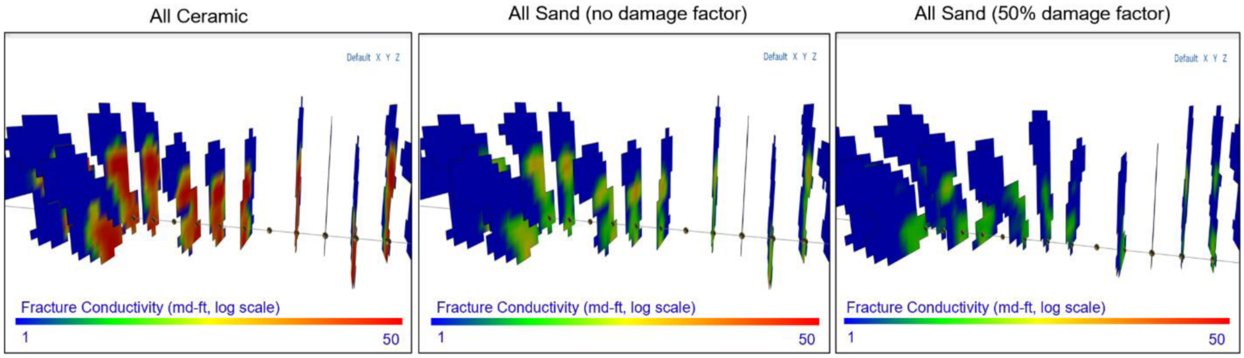

Figure 23—Fracture Conductivity After Three Years Of Production For Three Simulation Cases

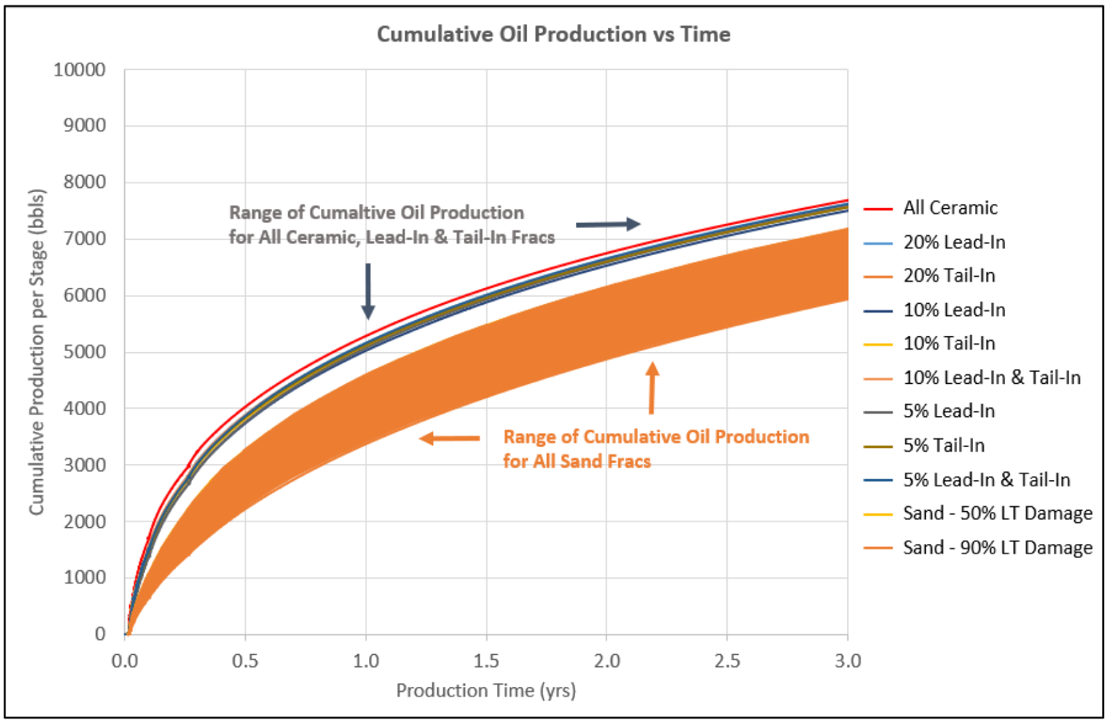

Figure 24—3-Year Cumulative Oil Plots for the Various Middle Bakken Fracture Designs

In order to calculate well payout times and cumulative free cash flow the pricing and cost data of Table 10 were used for analysis.

Table 10—Price and Cost Data Used In The Economic Analysis

Wellhead Pricing:	$50 / BO
	$2 / MMSCF
Royalty	18%
Production Taxes	10%
Well Cost (excluding proppant):	$5.038 Million
Proppant Costs:	Sand 5 c/lb
	Light Weight Ceramic 17 c/lb
	Last Mile Logistics 3 c/lb
Operating Costs:	$3 / BO fixed costs
	$2.25 / BW water disposal costs

The 3-year oil recovery results from Figure 23 are given in Table 11 together with the total well costs for each of the designs using the cost data from Table 10.

Table 11—3-Year Calculated Cumulative Oil Recovery for the Various Middle Bakken Fracture Designs

	Sand Pumped (lbs)	Ceramic Pumped (lbs)	Well Cost ($)	Well Cost Increase	3-Year Cumulative Oil (bbls)	% Oil Increase Over Avg. Sand Frac	Well Payout Period (Months)	Incremental 3-Year Cumulative Free Cash Flow Over Avg. Sand Frac (Million $)
All Sand - 50% LT Damage	10,936,728	-	$ 5,585,180	-	193,711	-	} 36	-
All Sand - 90% LT Damage	10,936,728	-	$ 5,585,180	-	162,102	-		-
5% LWC Lead-In	10,389,897	546,831	$ 5,650,800	1%	204,629	15%	25	0.75
5% LWC Tail-In	10,389,897	546,831	$ 5,650,800	1%	203,986	15%	25	0.70
5% LWC Lead-In & Tail-In	9,843,066	1,093,662	$ 5,716,420	2%	206,235	16%	26	0.73
10% LWC Lead-In	9,843,066	1,093,662	$ 5,716,420	2%	207,500	17%	26	0.74
10% LWC Tail-In	9,843,066	1,093,662	$ 5,716,420	2%	204,794	15%	26	0.65
10% LWC Lead-In & Tail-In	8,749,377	2,187,351	$ 5,847,662	5%	205,590	16%	27	0.55
20% LWC Lead-In	8,749,377	2,187,351	$ 5,847,662	5%	205,893	16%	27	0.56
20% LWC Tail-In	8,749,377	2,187,351	$ 5,847,662	5%	205,267	15%	27	0.54
All Ceramic	-	10,936,728	$ 6,897,588	23%	208,800	17%	43	-0.37

Table 11 also gives the well payout period and incremental 3-year cumulative free cash flow for each of the designs compared to the average sand frac case. As can be seen, payout time is reduced from ~36 months to a range of 25-27 months for each of the ceramic lead-in and tail-in designs. They also generate an incremental $0.54 Million to $0.75 Million cumulative cash flow. From the recovery results, it can be inferred that in all cases the pumping of 5% to 20% of the treatment as ceramic proppant is effectively propping the near-wellbore region and that this is the critical design factor since recovered volumes are in excess of 85% of that from an all ceramic design.

Production Over The Life of Well

Simulations were run out to 30-years of productive life and are presented in Figure 25 and Table 12. Clearly, as production rates decrease over the life of the well the need and benefit to increased conductivity is minimized - providing that the proppant pack does not totally plug due to fines generation and their migration / packing in the near-wellbore region. With that caveat, for all cases investigated here, where there is sustained residual fracture conductivity the total recovery between the average of the sand frac runs and all designs incorporating ceramic is a 4% difference in EUR.

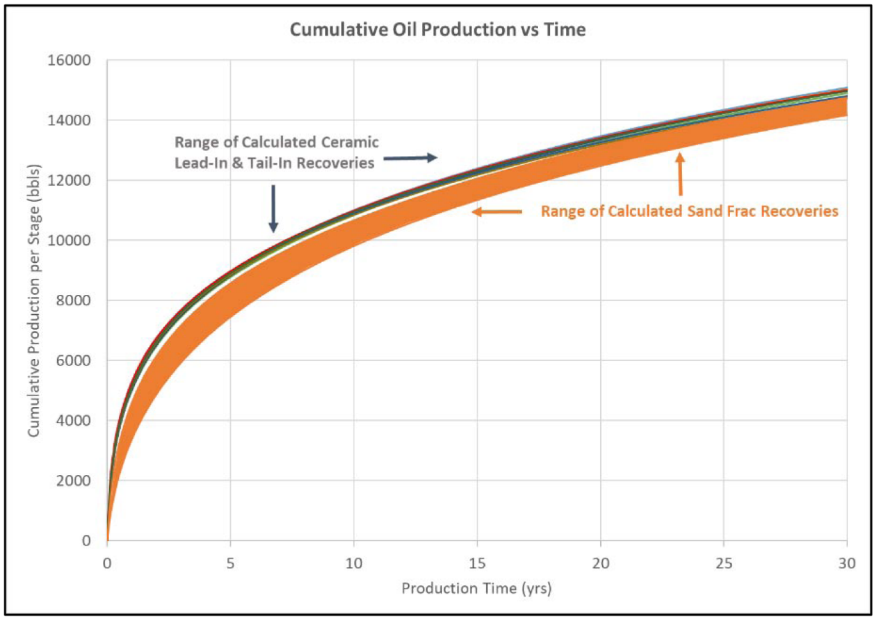

Figure 25—30-Year Cumulative Oil Plots for the Various Middle Bakken Fracture Designs

Table 12—30-Year Calculated Cumulative Oil Recovery for the Various Middle Bakken Fracture Designs

	Sand Pumped Per Stage (lbs)	Ceramic Pumped per Stage (lbs)	Cumulative Oil (bbls)	% Oil Increase Over All Sand Frac
All Sand	405,059	-	5,582	-
17% LWC Lead-In	330,089	69,300	6,293	13%
20% LWC Tail-In	320,059	85,000	6,052	8%
17% LWC Lead-In + 20% Tail-In	245,389	154,000	6,481	16%
All Ceramic	-	405,059	7,064	27%

Three Forks Simulation of Lead-Ins and Tail-Ins

Prior to having Middle Bakken production data from the Martin -3MBH well, a series of simulation runs were made evaluating larger lead-in and tail-in treatments in a Three Forks zone fracture treatment. Sensitivities were run using a 17% lead-in and 20% tail-in; and a combined Lead-In and Tail-In.

180-day production results are shown in Figure 26 and Table 13. While a similar increase in production is shown with the placement of high conductivity near-wellbore ceramic proppant what is of note is that the benefit of the lead-in material is greater than the benefit of the larger tail-in material. Figure 27 and Table 14 show the same effect occurring after 3-years of production. Since a significant amount of oil production is occurring from the higher Middle Bakken interval it is interpreted that the increased lead-in design performance is due to the increased near-wellbore conductivity as a result of proppant trapping occurring as height growth occurs during the lead-in stage – similar in concept to that observed in the slot flow tests from the lower injection port (Figure 11b).

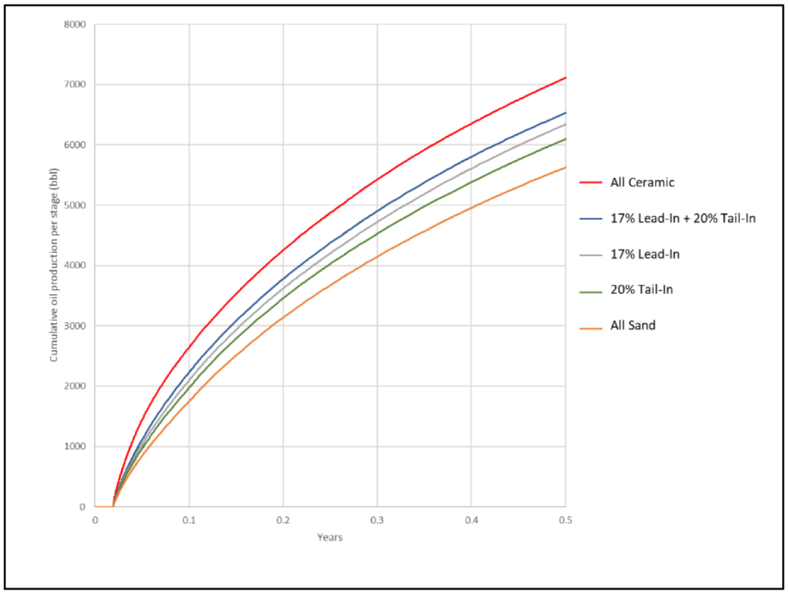

Figure 26—180-Day Cumulative Oil Plots for the Various Three Forks Fracture Designs

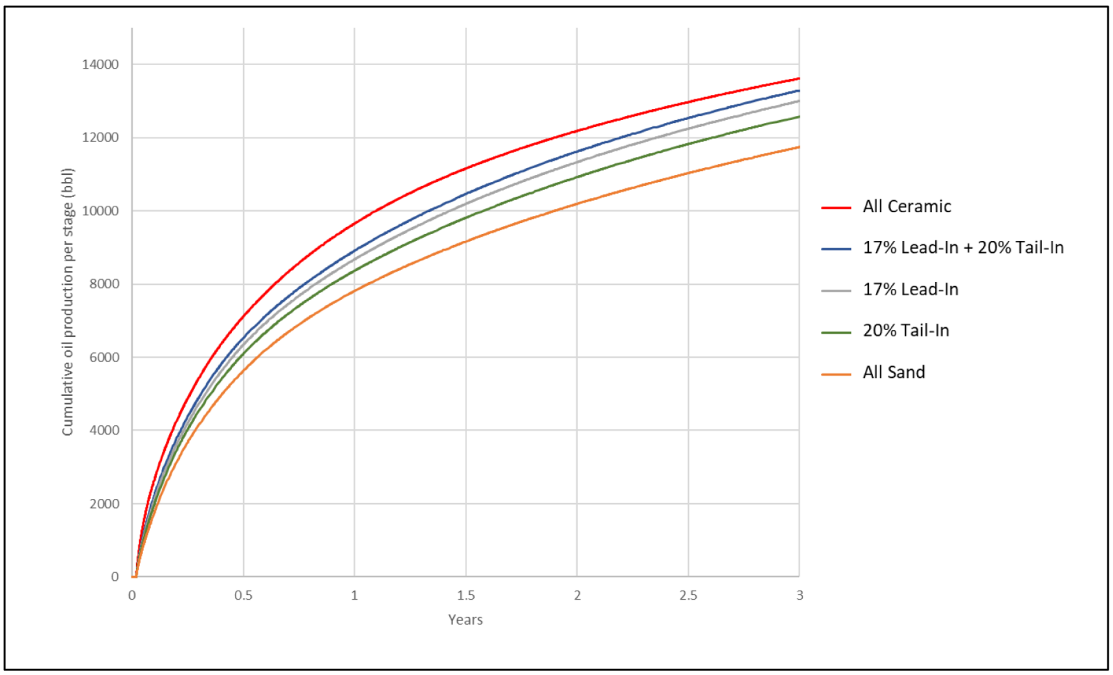

Figure 27—3-Year Cumulative Oil Plots for the Various Three Forks Fracture Designs

Table 13—180-Day Calculated Cumulative Oil Recovery for the Various Three Forks Fracture Designs

	Sand Pumped Per Stage (lbs)	Ceramic Pumped per Stage (lbs)	Cumulative Oil (bbls)	% Oil Increase Over All Sand Frac
All Sand	405,059	-	11,683	-
17% LWC Lead-In	330,089	69,300	12,937	11%
20% LWC Tail-In	320,059	85,000	12,516	7%
17% LWC Lead-In + 20% Tail-In	245,389	154,000	13,229	13%
All Ceramic	-	405,059	13,562	16%

Table 14—3-Year Calculated Cumulative Oil Recovery for the Various Three Forks Fracture Designs

	Sand Pumped Per Stage (lbs)	Ceramic Pumped per Stage (lbs)	Cumulative Oil (bbls)	% Oil Increase Over All Sand Frac
All Sand	405,059	-	11,683	-
17% LWC Lead-In	330,089	69,300	12,937	11%
20% LWC Tail-In	320,059	85,000	12,516	7%
17% LWC Lead-In + 20% Tail-In	245,389	154,000	13,229	13%
All Ceramic	-	405,059	13,562	16%

After 30-years of production all designs cum'd ~670 MBO as in this study there was no long-term proppant damage assessed to either type of proppant.

It should be noted that this series of simulations did not include any history matching but rather used the log-derived formation permeability values and thus resulted in EURs that are 50% above what the company currently achieves in the East Nesson area. Nevertheless, the relative impacts of the different designs are still relevant and the 670 MBO EUR is more typical of the company's Tier 1 acreage.

Conclusions

The petroleum industry has continued to innovate and advance the application of hydraulic fracturing over the past 60 years. The most recent 15-years has seen a paradigm shift in the exploitation of unconventional oil and gas reservoirs through the combination of horizontal drilling with multi-stage hydraulic fracturing to generate a well production system comprised of multitudes of transverse hydraulic fractures.

Both the short-term and longer-term production performance of a multi-stage hydraulically fractured well are controlled by the near-wellbore fracture pack conductivity and its connectivity to the wellbore. Using a combination of high conductivity ceramic proppant lead-in and tail-in stages to generate that conductivity is shown from laboratory studies to be feasible to place near-wellbore in the fracture, and from numerical simulation and actual production data to generate significant economic return. This occurs through both an increase in early-time production generating an immediate payout of the proppant cost and faster payout of the entire well, while also providing the increased conductivity to minimize the effects of proppant degradation due to time at stress and fines migration associated with sand crushing in the body of the fracture.

In the case of a single zone being fractured and exhibiting significant height growth into non-productive pay it was found that a tail-in design generated greater production benefit compared to a lead-in of the same proppant mass. For the case of a well design that is draining oil from an upper zone it was found that a lead-in design generated greater productivity than a tail-in.

A variety of simulations run with 5 to 10% ceramic proppant as a lead-in and/or a tail-in generated a combination of very positive economic results:

– payout of the incremental ceramic proppant costs in 1 to 2 months of increased production;
– a significantly reduced payout of the entire well cost from ~36 months with an all sand stimulation design to 25-27 months for the ceramic lead-in and tail-in designs; and
– an increase in 3-year cumulative free cash flow of $0.54 to $0.75 Million

Finally, it is recognized that the economic results are highly dependent on the long-term effective permeability of the proppant pack. In this study we have used the most realistic assessment of extended-term reference conductivity testing from existing industry data and then made assumptions on the longer-term impacts commensurate with other observed field evaluations of proppant performance. Clearly, more data are needed by industry to quantify the extended-time properties for all proppant types and especially sand proppants due to their propensity to show significant crush and generation of fines.

The use of 50-hour reference conductivity data to justify a "one size fits all" design strategy of pumping the lowest cost proppant is likely having significant detrimental economic impact on the industry's performance over the life of the well – including the payout period of the well investment and cumulative free cash flow in the first 3-years of production.

Acknowledgements

The authors are appreciative of their company's management for granting permission to publish and their co-workers for their many hours of hard work and support in conducting the studies.

References

Al-Tailji, (2018). The Importance of Contact, Conductivity, and Connectivity in Multi-Fractured Horizontal Wells. Society of Petroleum Engineers Distinguished Lecture Series 2017/18.

API RP 56 (1983/1995). Recommended Practices for Testing Sand Used in Hydraulic Fracturing Operations; Washington D.C., American Petroleum Institute.

API RP 60 (1989/1995). Recommended Practices for Testing High-Strength Proppants Used in Hydraulic Fracturing Operations; Washington D.C., American Petroleum Institute.

API RP 61 (1989). Recommended Practices for Evaluating Short Term Proppant Pack Conductivity, Washington D.C., American Petroleum Institute.

API STD 19C (2007/2018); Measurement of and Specifications for Proppants Used in Hydraulic Fracturing and Gravel Packing Operations, Washington D.C., American Petroleum Institute.

API RP 19D (2008). Recommended Practices for Measuring the Long Term Conductivity of Proppants; Washington D.C., American Petroleum Institute.

Barree, R. D., Cox, S. A., Barree, V. L., & Conway, M. W. (2003, January 1). Realistic Assessment of Proppant Pack Conductivity for Material Selection. Society of Petroleum Engineers. doi: 10.2118/84306-MS

Becq, D. F., Claude, R., & Sarda, J. P. (1984, January 1). High-Strength Proppants Behavior Under Extreme Conditions. Society of Petroleum Engineers. doi: 10.2118/12487-MS

Cobb, S. L., & Farrell, J. J. (1986, January 1). Evaluation of Long-Term Proppant Stability. Society of Petroleum Engineers. doi: 10.2118/14133-MS

Cooke, C.E. Jr., Hedden, W.A., and Chard, W.C.: "Hydraulic Fracturing Method Using Sintered Bauxite Proppant Agent," U.S. Patent No. 4,068,718 (1978).

Cooke, C. E. (1975, October 1). Effect of Fracturing Fluids on Fracture Conductivity. Society of Petroleum Engineers. doi: 10.2118/5114-PA

Coulter, G. R., Benton, E. G., & Thomson, C. L. (2004, January 1). Water Fracs and Sand Quantity: A Barnett Shale Example. Society of Petroleum Engineers. doi: 10.2118/90891-MS

Duenckel, R. J., Barree, R. D., Drylie, S., O'Connell, L. G., Abney, K. L., Conway, M. W., Chen, F. (2017, October 9). Proppants - What 30 Years of Study has Taught Us. Society of Petroleum Engineers. doi: 10.2118/187451-MS

Economides, M.J. and Martin, T, 2007. *Modern Fracturing Enhancing Natural Gas Production*, p.301.

Ely, J. W., Harper, J., Nieto, E. N., & Semmelbeck, M. (2019, January 29). CounterProp, Finally Adding the Correct Proppant in the Proper Size and Proper Sequence in Slick Water Treatments. Society of Petroleum Engineers. doi: 10.2118/194370-MS

Fischer, D. W., J. A. LeFever, J. A. Sorensen, S. A. Smith, L. D. Helms, R. D. LeFevre, S. G. Whittaker, E. N. Steadman, and J. A. Harju, 2005, The influence of tectonics on the potential leakage of CO2 from deep geological sequestration units in the Williston Basin: Plains CO2 Reduction (PCOR) Partnership, 17 p.

Fitzgibbon, J.J.: "Sintered Spherical Pellets Containing Clay as a Major Component Useful for Gas and Oil Well Proppants," U.S. Patent No. 4,427,068 (1984).

Fowler, G., McClure, M., & Cipolla, C. (2019, September 23). A Utica Case Study: The Impact of Permeability Estimates on History Matching, Fracture Length, and Well Spacing. Society of Petroleum Engineers. doi: 10.2118/195980-MS

Fowler, G., McClure, M. & Allen, J. (2020). RTA Assisted History Matching with a Combined Hydraulic Fracturing and Reservoir Simulator. Paper SPE-199149-MS presented at the SPE Virtual Latin American and Caribbean Petroleum Engineering Conference.

Gale, J. F. W., Elliott, S. J., & Laubach, S. E. (2018). Hydraulic fractures in core from stimulated reservoirs: Core fracture description of the HFTS slant core, Midland Basin, West Texas. Paper presented at the Unconventional Resources Technology Conference, Houston, TX.

Handren, P. J., & Palisch, T. T. (2007, January 1). Successful Hybrid Slickwater Fracture Design Evolution--An East Texas Cotton Valley Taylor Case History. Society of Petroleum Engineers. doi: 10.2118/110451-MS

Handren, P., Pearson, C. M., Kullman, J., Coleman, R. J., Foreman, J., Froebel, K., & Caron, J. (2001, January 1). The Impact of Non-Darcy Flow on Production from Hydraulically Fractured Gas Wells. Society of Petroleum Engineers. doi: 10.2118/67299-MS

Heck, T.J., R. D. LeFever, D. W. Fischer, and J. LeFever, 2004, Overview of the petroleum geology of the North Dakota Williston Basin: North Dakota Geological Survey, https://www.dmr.nd.gov/ndgs/Resources

Howard, G.C. and Fast, C.R.: Hydraulic Fracturing, Monograph Series, SPE, Richardson, TX (1970) 59-90.

Graham, J.W. et al: "Method for Treating Subterranean Formations," U.S. Patent No. 3,929,191 (1975).

Johnson, C.K. and Armbruster, D.R.: "Particles Covered with a Cured Infusable Thermoset Film and Process for Their Production," U.S. Patent No. 4,439,489 (1984).

Kern, L. R., Perkins, T. K., & Wyant, R. E. (1959, July 1). The Mechanics of Sand Movement in Fracturing. Society of Petroleum Engineers. doi: 10.2118/1108-G

Lunghofer, E.P.: "Hydraulic Fracturing Propping Agent," U.S. Patent No. 4,522,731 (1985)

Maity, D., & Ciezobka, J. (2020, January 28). A Data Analytics Framework for Cored Fracture Imaging and Novel Characterization Workflow - Application on Samples from Hydraulic Fracturing Test Site HFTS in the Midland Basin. Society of Petroleum Engineers. doi: 10.2118/199754-MS

Mayerhofer, M. J., Richardson, M. F., Walker, R. N., Meehan, D. N., Oehler, M. W., & Browning, R. R. (1997, January 1). Proppants? We Don't Need No Proppants. Society of Petroleum Engineers. doi: 10.2118/38611-MS

McClure, M., Kang, C., Hewson, C., and Medam, S. (2020a). ResFrac Technical Writeup. arXiv:1804.02092.

McClure, M., Picone, M., Fowler, G., Ratcliff, D., Kang, C., Medam, S., & Frantz, J. (2020b). Nuances and frequently asked questions in field-scale hydraulic fracture modeling. SPE-199726-MS. Paper presented at the SPE Hydraulic Fracturing Technology Conference and Exhibition, The Woodlands, TX.

Melcher, H., Mayerhofer, M., Agarwal, K., Lolon, E., Oduba, O., Murphy, J., Weijers, L. (2020, January 28). Shale Frac Designs Move to Just-Good-Enough Proppant Economics. Society of Petroleum Engineers. doi: 10.2118/199751-MS

Milton-Tayler, D. (1993, January 1). Realistic Fracture Conductivities of Propped Hydraulic Fractures. Society of Petroleum Engineers. doi: 10.2118/26602-MS

Miskimins, J.L., 2019. Hydraulic Fracturing: Fundamentals and Advancements; pp.143-164. Society of Petroleum Engineers; ISBN: 978-1-61399-719-2.

Montgomery, C. T., & Steanson, R. E. (1985, December 1). Proppant Selection: The Key to Successful Fracture Stimulation. Society of Petroleum Engineers. doi: 10.2118/12616-PA

Much, M. G., & Penny, G. S. (1987, January 1). Long-Term Performance of Proppants Under Simulated Reservoir Conditions. Society of Petroleum Engineers. doi: 10.2118/16415-MS

Olmen, B. (2019, March 4). 2018 Proppant Market Report. Published by Proptester Inc. and Kelrik LLC.

Palisch, T. T., Duenckel, R. J., Bazan, L. W., Heidt, J. H., & Turk, G. A. (2007, January 1). Determining Realistic Fracture Conductivity and Understanding its Impact on Well Performance - Theory and Field Examples. Society of Petroleum Engineers. doi: 10.2118/106301-MS

Palisch, T. T., Vincent, M. C., & Handren, P. J. (2008, January 1). Slickwater Fracturing: Food for Thought. Society of Petroleum Engineers. doi: 10.2118/115766-MS

Pearson, C. M. (2002, January 1). The ABC's of Improving Production from Hydraulically Fractured Wells. Society of Petroleum Engineers. SPE 101454-DL.

Renkes, I., Anschutz, D., Sutter, K., & Rickards, A. (2017, January 24). Long Term Conductivity vs. Point Specific Conductivity. Society of Petroleum Engineers. doi: 10.2118/184814-MS

Sonnenburg, S. A, Gantyno, A., and Sarg, R., 2011, Petroleum Potential of the Upper Three Forks Formation, Williston Basin, USA: U.S. Active and Emerging Plays--Paleozoic Basins and Cretaceous of Rockies, AAPG Annual Convention and Exhibition, Houston, Texas, USA

Vincent, M. C. (2002, January 1). Proving It - A Review of 80 Published Field Studies Demonstrating the Importance of Increased Fracture Conductivity. Society of Petroleum Engineers. doi: 10.2118/77675-MS

Vincent, M. C., & Besler, M. R. (2013, August 12). Declining Frac Effectiveness - Evidence that Propped Fractures Lose Conductivity, Surface Area, and Hydraulic Continuity. Unconventional Resources Technology Conference. doi: 10.1190/urtec2013-073

Vincent, M. C. (2009, January 1). Examining Our Assumptions -- Have Oversimplifications Jeopardized Our Ability to Design Optimal Fracture Treatments? Society of Petroleum Engineers. doi: 10.2118/119143-MS

Vincent, M. C., Pearson, C. M., & Kullman, J. (1999, January 1). Non-Darcy and Multiphase Flow in Propped Fractures: Case Studies Illustrate the Dramatic Effect on Well Productivity. Society of Petroleum Engineers. doi: 10.2118/54630-MS

Weijers, L., Wright, C., Mayerhofer, M., Pearson, M., Griffin, L., & Weddle, P. (2019, January 29). Trends in the North American Frac Industry: Invention through the Shale Revolution. Society of Petroleum Engineers. doi: 10.2118/194345-MS